Desalination 250 (2010) 249–256

Contents lists available at ScienceDirect

Desalination

journal homepage: www.elsevier.com/locate/desal

Comparison of classical solar chimney power system and combined solar chimney system for power generation and seawater desalination

Xinping Zhou [a], Bo Xiao [b,1], Wanchao Liu [b], Xianjun Guo [b,1], Jiakuan Yang [b,2], Jian Fan [a,*]

[a] School of Civil Engineering and Mechanics, Huazhong University of Science and Technology, 1037 Luoyu Road, Wuhan, Hubei 430074, China
[b] School of Environmental Science and Engineering, Huazhong University of Science and Technology, 1037 Luoyu Road, Wuhan, Hubei 430074, China

ARTICLE INFO

Article history:
Accepted 9 March 2009
Available online 23 October 2009

Keywords:
Solar chimney
Power generation
Seawater desalination
Water generator

ABSTRACT

An alternative method of heat and moisture extraction from seawater under the collector of a solar chimney system for power generation and seawater desalination is investigated with the aim of estimating the output of power and fresh water when used in seawater desalination using one-dimensional compressible flow model. It is found that the temperature and velocity of the airflow inside the chimney in the combined plant is less than that inside the chimney in the classic plant due to the release of vapor latent heat as the air rises up the chimney. Additionally, the power output from air turbine generators and water generators in the combined plant is less than that of the classic plant. Furthermore, a revenue analysis based on the price of fresh water and electric power in Dalian, China shows that the chimney less than 445 m high for the proposed combined solar chimney power plant having a collector 3000 m in radius is more economical than for the classic plant. The critical chimney height is found to depend on the local price of fresh water and electricity.

1. Introduction

Water and energy are two inseparable items in our lives [1]. In recent years, both energy crisis and fresh water shortage problem posing great threat to the humans are attracting great importance around the world owing to rapid development of global economy, fresh water pollution, increase in population, and improvement of living standards. Seawater desalination is one of the prevalent methods of obtaining large amounts of fresh water. Renewable energy driven desalination systems have been extensively discussed as an innovative approach to desalinate economically in an environmentally friendly manner [1,2]. Delyannis reviewed desalination using renewable energy with special reference to the use of solar energy for desalination [1]. The use of solar energy in distillation can go back to medieval times. Recently, some investigations were carried out [3–13] and some plants (e.g. the Las Salinas distillation plant [14], the Patmos distillation plant [15], the Coober–Pedy distillation plant [16], the Abu–Dhabi MED plant [17]) were built up. Pereira et al. [18–20] designed and tested an advanced solar dryer for salt recovery from brine effluent of an MED desalination plant which consists of solar collectors and a chimney. This chimney producing airflow accelerates evaporation of water and helps desalination in the collector. This chimney is also used in solar chimney power plant which was first described in a publication written by a German author, Gunther in 1931 [21]. Classical solar chimney power system (CSCS) (see Fig. 1), designed to produce electric power on a large scale [22,23], utilizes solar energy to produce ventilation that drives air turbine generators to produce electric power. The technology combines three components: a collector, a chimney and air turbines [22]. In the collector, solar radiation is used to heat an absorber (ordinarily soil or water bags [24]) on the ground, and then a large body of air, heated by the absorber, rises up the chimney, due to the density difference from the air inside the chimney and the ambient air. The rising air drives air turbine generators installed at the chimney base to generate electricity. Since again proposed by Schlaich in 1978, some investigations were done [25–45] and some pilot setups (e.g. the Manzanares prototype plant [22,46,47], the Connecticut setup [48], the Izmit setup [49], the Florida setup [50], the Wuhan setup [40], the Botswana setup [51], and the Brazil setup [52]) were built up and tested.

In a view of the above, a novel concept using solar chimney system to drive both power generation and seawater desalination suitably at a site adjacent to the sea was proposed by Wang et al. [53]. In the new system, seawater pumped from the sea opens to air in the collector where warm and saturated operating air is produced by solar energy. The vapor contained in the warm air inside the chimney is condensed to water using a high-efficiency condenser installed at the chimney top, and fresh water holding big gravitational potential energy is used for power generation through water turbine generators installed at ground level. The products from the power plant include electric power from air turbine generators and water turbine generators and fresh water, though the electric power from air turbine generators is far less than the same-scale CSCS due to buoyancy being smaller because much heat is used as latent heat of water evaporation [29]. Additionally, the performances of the two systems change at different sites where there are different climatic conditions and prices of electricity and fresh water

* Corresponding author. Tel.: +86 27 62250811; fax: +86 27 87542221.
E-mail addresses: xpzhou08@mail.hust.edu.cn (X. Zhou), fan-jian@126.com (J. Fan).
[1] Tel.: +86 27 87557464; fax: +86 27 87792101.
[2] Tel.: +86 27 87792207; fax: +86 27 87792101.

0011-9164/$ – see front matter
doi:10.1016/j.desal.2009.03.007

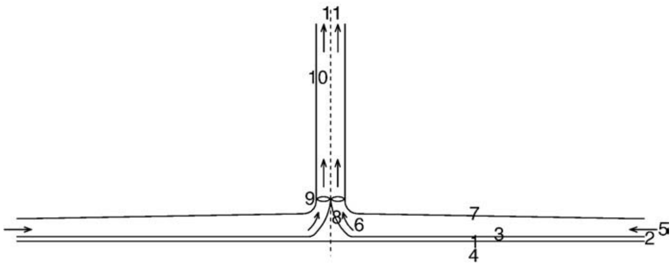

Fig. 1. Schematic diagram of CSCS. 1: Black absorber; 2: Water layer; 3: Transparent plastic film; 4: Thermal resistance bed and ground; 5: Cool ambient air; 6: Hot operating air; 7: Transparent cover; 8: Guiding cone; 9: Air turbines; 10: Chimney; 11: Chimney outlet airflow.

in the market. So, there is a better choice between the combined system and CSCS to maximize the revenue of products at a given site.

In this paper, by using a mathematical model on energy balance, theoretical analyses are carried out to investigate the performance of combined solar chimney system for power generation and seawater desalination (CSCSPD), and revenue analysis is made to compare the results with those of CSCS.

2. Description of CSCSPD

The CSCSPD is shown in Fig. 2. The power generation–seawater desalination coupling scheme is very suitable for regions adjacent to the sea or natural alkaline lakes. The combined system consists of four components, i.e. the solar collector, the solar chimney, the turbine generators, and the high-efficiency condenser. The influence of the high efficiency condenser on the outflow of the up drafting air in the solar chimney is not considered. Unlike classical solar collector, the absorber bed under solar collector is seawater open to operating air. It works as a producer of warm air and vapor. The condenser is installed at the chimney top.

In the system, the dry ambient air becomes warm and saturated when it flows through a layer of seawater drawn from the adjacent sea. Resulting from a sum of heat wasted in vapor latent heat, the saturated air is colder than that produced in CSCS under the same conditions. This results in the reduction in driving force and the power generated. The temperature of the warm and saturated air decreases a little when the air rises from the bottom to the top of the chimney where a little vapor is condensed to the fresh water. The low trough around the guiding cone is used to receive the fresh water falling from a high height in the chimney. The fresh water in the low trough is then drawn out continuously. The warm and saturated air enters directly into the high-efficiency condenser

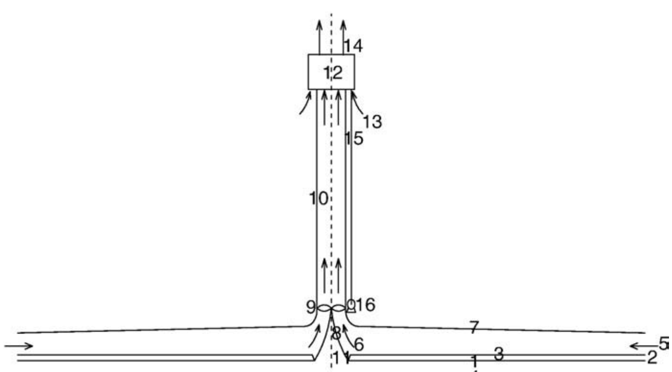

Fig. 2. Schematic diagram of CSCSPD. 1: Black absorber; 2: Seawater layer; 3: Seawater surface; 4: Thermal resistance bed and ground; 5: Cool and dry ambient air; 6: Warm and saturated operating air; 7: Transparent cover; 8: Guiding cone; 9: Air turbines; 10: Chimney; 11: Water falls trough; 12: High-efficiency condenser; 13: Cool and dry ambient air around the chimney outlet; 14: Warmed ambient air; 15: Condensation water; 16: Water generator.

after flowing out from the chimney. Cold ambient air around the chimney outlet naturally enters the condenser due to pressure difference. In the condenser, vapor contained in the saturated air is condensed due to the effect of cold ambient air, to produce fresh water. This condensation occurs, naturally, and needs no extra energy. The fresh water falls and drives the water generators installed above the collector to generate electricity, converting gravitational potential energy of water to electric power. The little fresh water drawn out from the low trough and large amounts falling from the water generator will supply the local needs of fresh water after a simple treatment.

3. Mathematical model

A mathematical model formulated by coupling the energy balance equations of components of the systems is now discussed. The model is used to evaluate the performance of CSCSPD. The model is based on the following assumptions,

1. The air follows the ideal gas law.
2. Only the buoyancy force is considered in solar chimney system.
3. The chimney wall is considered to be adiabatic and slippery.
4. The performance of airflow doesn't change when it goes through the turbine by neglecting the influence of turbine.

3.1. One-dimensional flow in the collector

3.1.1. For classical solar chimney system

The absorber of CSCSs may be natural ground heat storage system or additional water heat storage system. In the study, additional water heat storage system with a water layer covered by a transparent plastic film [28] is selected.

Solar collectors include single channel collector and double channel collector. The energy balance for the components of CSCS with double channel collector was developed by Bernardes et al. [28]. One-dimensional equations of energy balance to the control volume from a radius r to $r+\Delta r$ for the components of CSCS can be expressed as,

For a black absorber,

$$(\tau_1\tau_2\alpha_3)'S = h_{ab,wa}(T_{ab}-T_{wa}) + h_{r,ab,p}(T_{ab}-T_p) + U_b(T_{ab}-T_g). \quad (1)$$

For water,

$$h_{ab,wa}(T_{ab}-T_{wa}) = h_{wa,p}(T_{wa}-T_p). \quad (2)$$

For transparent plastic film,

$$\begin{aligned}&(\tau_1\alpha_2)'S + h_{r,ab,p}(T_{ab}-T_p) + h_{wa,p}(T_{wa}-T_p)\\ &\quad = h_{p,f}(T_p-T_f) + h_{r,p,c}(T_p-T_c).\end{aligned} \quad (3)$$

For dry operating air,

$$\frac{dT_f}{dr} = \frac{h_{p,f}(T_p-T_f) - h_{f,c}(T_f-T_c)}{\dot{m}_f c_p} 2\pi r \quad (4)$$

with $T_f\,(R_{coll}) = T_a$,and for transparent cover film,

$$\alpha_1 S + h_{f,c}(T_f-T_c) + h_{r,p,c}(T_p-T_c) = U_t(T_c-T_a) \quad (5)$$

where, S is solar radiation; τ_1 and τ_2 are respectively transparent cover film and transparent plastic film transmissivity; α_1, α_2 and α_3 are respectively transparent cover film absorptivity, transparent plastic film absorptivity and black absorber absorptivity.

3.1.2. For combined system used for power generation and seawater desalination

The energy conversion and heat transfer of the power generation–seawater desalination coupling system are complex, and can be divided into six phases: In the first phase, solar radiation heats seawater. In the second phase, hot seawater heats the entering ambient air and produces the evaporation of water by providing vapor latent heat, with warm and saturated air produced. In the third phase, the chimney which acts as a thermal engine drives warm operating air. In the fourth phase, the turbine generators in turn convert airflow in form of kinetic energy to electric power when air flows through the turbines. In the fifth phase, vapor contained in the warm saturated air is condensed to fresh water in the high-efficiency condenser. In the sixth phase, fresh water falls off and drives the water generators installed above the collector to generate electricity, converting gravitational potential to electric power.

The equations of energy balance to the control volume from a radius r to $r+\Delta r$ for the components in the collector can be expressed as,

For a black absorber,

$$(\tau_1\alpha_2)S = h_{ab,se}(T_{ab}-T_{se}) + h_{r,ab,c}(T_{ab}-T_c) + U_b(T_{ab}-T_g). \tag{6}$$

For seawater,

$$h_{ab,se}(T_{ab}-T_{se}) = h_{se,f}(T_{se}-T_f) + \frac{L}{2\pi r}\frac{d\dot{m}_{va}}{dr}. \tag{7}$$

For warm saturated operating air,

$$\frac{dT_f}{dr} = \frac{h_{se,f}(T_{se}-T_f) - h_{f,c}(T_f-T_c)}{\dot{m}_f\, c_p}2\pi r \tag{8}$$

with $T_f(R_{coll}) = T_a$, and for transparent cover film,

$$\alpha_1 S + h_{f,c}(T_f-T_c) + h_{r,ab,c}(T_{ab}-T_c) = U_t(T_c-T_a). \tag{9}$$

The sky temperature, T_{sky}, is given by Swinbank [54] as,

$$T_{sky} = 0.0552T_a^{1.5}. \tag{10}$$

The mass flow rate of operating air passing through the collector outlet is equal to that through the chimney inlet, $\dot{m}_f$, which can be calculated with the help of the following equation,

$$\dot{m}_f = \rho_{ch,in}\cdot A_c\cdot u_{ch,in}. \tag{11}$$

Whereas the latent heat of water evaporation, L, is given by,

$$L = 2502535.259 - 212.56384T. \tag{12}$$

The mass flow rate of vapor evaporated from the surface of seawater, $\dot{m}_{va}$, is given by,

$$\dot{m}_{va} = \dot{m}_f d_1$$

The moisture content of wet air is,

$$d = \frac{\rho_v}{\rho_d} = 0.622\frac{p_v}{p-p_d}. \tag{14}$$

The saturated vapor pressure can be expressed by Zhou et al. [55] as,

$$P_{sv} = P_{sv0}\cdot 10^{8.5(T-273.15)/T} \tag{15}$$

where the saturated vapor pressure at 0 °C, P_{sv0}, is equal to 608.2 Pa.

The specific heat capacity of wet air, c_p, is expressed as,

$$c_p = 1010 + 1880d \tag{16}$$

where $h_{r,ab,c}$ $h_{r,ab,p}$ $h_{r,p,c}$ denote radiation heat transfer coefficient from absorber to cover, heat transfer coefficient from absorber to plastic film, and heat coefficient transfer from plastic film to cover, respectively. These quantities can be expressed in the following compact form

$$h_{r,1,2} = \frac{\sigma(T_1^2+T_2^2)(T_1+T_2)}{1/\varepsilon_1 + 1/\varepsilon_2 - 1} \tag{17}$$

with $h_{ab,wa}$, $h_{ab,br}$ and $h_{wa,p}$ denoting convection heat transfer coefficient from absorber to water layer, from absorber to seawater layer, and from water layer to plastic film, respectively. These are calculated according to the equations used by Bernardes et al. [28].

The chimney acts as a thermal engine, which forces air to flow between the cover and the black plastic film. The air flow inside the collector is considered to be natural convection and forced convection effects. $h_{se,f}$, $h_{p,f}$ and $h_{f,c}$ denote the convection heat transfer coefficient from seawater surface to operating air due to wind, from the plastic film to internal airflow, and from the internal airflow to the cover, respectively. The equations governing them are given by Pretorius and Kröger [36] as,

$$h_{se,f} = \frac{0.2106 + 0.0026v_f\left(\rho T_m/\mu g(T_{se}-T_f)\right)^{1/3}}{\left(\mu T_m/g(T_{se}-T_f)c_p k^2\rho^2\right)^{1/3}} \tag{18}$$

$$h_{p,f} = \frac{0.2106 + 0.0026v_f\left(\rho T_m/\mu g(T_p-T_f)\right)^{1/3}}{\left(\mu T_m/g(T_p-T_f)c_p k^2\rho^2\right)^{1/3}} \tag{19}$$

$$h_{f,c} = \frac{0.2106 + 0.0026v_f\left(\rho T_m/\mu g(T_f-T_c)\right)^{1/3}}{\left(\mu T_m/g(T_f-T_c)c_p k^2\rho^2\right)^{1/3}}. \tag{20}$$

According to ref [56], the top loss coefficient, U_t, is expressed as,

$$U_t = U_{t,p}\cdot\frac{T_p-T_a}{T_c-T_a} \tag{21}$$

where,

$$U_{t,p} = \frac{1}{\frac{1}{1.2529}\left(\frac{T_p-T_a}{1.76-0.118v_w+0.0066v_w^2}\right)^{-0.25} + \frac{1}{2.8+3\cdot v_w}} + \frac{\sigma(T_p^2+T_a^2)(T_p+T_a)}{\varepsilon_p^{-1} + \frac{1+ff}{\varepsilon_p} - 1}. \tag{22}$$

The bottom heat loss coefficient, U_b, is given by,

$$U_b = 1/(d_r/k_r + 1/U_g) \tag{23}$$

where, d_r and k_r are the thickness and thermal conductivity of thermal resistance bed. The ground loss coefficient, U_g, is given by Bernardes et al. [28] as,

$$U_g = 2\sqrt{\frac{k_g\rho_g c_{p,g}}{\pi\cdot t}}. \tag{24}$$

In this model, a mean value for a period of 86,400 s is used in the energy calculation in a day, and T_g is assumed to be equal to T_a.

3.2. One-dimensional compressible flow in the chimney

When warm and saturated air rises up a solar chimney in CSCS, the result is a reduction in temperature, and condensation of vapor of mass flow $\delta\dot{m}$ to water takes place otherwise, $\delta\dot{m}$ would be 0 when dry air rises up the solar chimney in CSCSPD.

One-dimensional equations to the control volume from a height h to $h+\Delta h$ may be expressed as,

For the state,

$$\frac{dp}{p} = \frac{dT}{T} + \frac{d\rho}{\rho}. \tag{25}$$

For the mass,

$$\frac{d\rho}{\rho} + \frac{du}{u} = 0. \tag{26}$$

For the momentum,

$$dp + \rho u du + \rho g dh = 0 \tag{27}$$

which may further be expressed as,

$$\frac{dp}{p} + \gamma Ma^2\left(\frac{du}{u} + \frac{gdh}{u^2}\right) = 0. \tag{28}$$

The energy equation takes the form

$$-dI(\dot{m}_f(h) - \delta\dot{m}) + L\delta\dot{m} = (\dot{m}_f(h) - \delta\dot{m})gdh \tag{29}$$

where, I is the specific enthalpy given by

$$I = c_pT + u^2/2 = c_pT_0 \tag{30}$$

with, T_0 is the stagnation temperature. $\delta\dot{m}$ is negligible compared with $\dot{m}_f$, and $\dot{m}_f(h)$ can be considered as a constant. Eq. (29) can therefore be simplified as,

$$dI = \frac{L\delta\dot{m}}{\dot{m}_f} - gdh = \delta\dot{Q}(h) - gdh. \tag{31}$$

Substituting Eq. (30) into Eq. (31) one obtains,

$$\frac{\delta Q(h) - gdh}{c_p^2} = \frac{1}{\gamma-1}\frac{dT}{T} + Ma^2\frac{du}{u} \tag{32}$$

Substituting Eqs. (25), (26), (28) into Eq. (32), Eq. (32) reduces to

$$\begin{aligned}\frac{\delta Q(h) - gdh}{c_p^2} &= \frac{1}{\gamma-1}\left(\left(1-Ma^2\right)\frac{du}{u} - \frac{rgdh}{c_p^2}\right)\\ &= \frac{1}{\gamma-1}\left(\left(1-Ma^2\right)\frac{dMa}{Ma} - \frac{gdh}{c_p^2}\right)\end{aligned} \tag{33}$$

where, $\frac{dMa}{Ma}$ can be expressed from Eq. (33) as,

$$\frac{dMa}{Ma} = \frac{(\gamma-1)\delta Q(h) + gdh}{c^2(1-Ma^2)}. \tag{34}$$

Mach number of the chimney outlet airflow, Ma_2, can be calculated with the help of the following equation,

$$\ln Ma_2 - \frac{1}{2}Ma_2^2 = \frac{r-1}{c_p^2}\Delta Q(H) + \frac{g}{c_p^2}H + \ln Ma_1 - \frac{1}{2}Ma_1^2. \tag{35}$$

Eq. (31) then becomes,

$$c_pdT_0 = \delta Q(z) - gdh. \tag{36}$$

Integrating Eq. (36) from $h=0$ to a height h leads to,

$$c_pT_0 = \Delta Q(h) - gh + c_pT_{01}. \tag{37}$$

The stagnation temperature of the chimney outlet airflow, T_{02}, is therefore expressed as,

$$T_{02} = \Delta Q(H)/c_p - gH/c_p + T_{01}. \tag{38}$$

The static temperature of the chimney outlet airflow is then calculated from,

$$T_2 = T_{02}/\left(1 + Ma_2^2(\gamma-1)/2\right). \tag{39}$$

A relation between p_2 and p_1 as expressed by von Backström and Gannon [27] following from the mass flow equation is

$$\frac{p_2}{p_1} = \frac{Ma_1}{Ma_2}\left(\frac{T_2}{T_1}\right)^{0.5} \tag{40}$$

where, p_2 is equal to the ambient static pressure at the same height, p_{a2}. When the height is below 11,000 m, p_{a2} is given by Zhao et al. [57] as,

$$p_{a2} = p_{a0}\left(1 - \frac{H}{44300}\right)^{5.256}. \tag{41}$$

When the mass flow rate of vapor contained in the saturated air, $\Delta\dot{m}_{water1}$, is condensed, vapor latent heat released, ΔQ, is calculated from,

$$\Delta Q = L\Delta\dot{m}_{water1} \tag{42}$$

where, $\Delta\dot{m}_{water1}$ can be approximately calculated from,

$$\Delta\dot{m}_{water1} = \dot{m}_f\frac{d_1}{1+d_1} - \dot{m}_f\frac{d_2}{1+d_2} \tag{43}$$

by assuming all of extra vapor contents in supersaturated air is condensed, theoretically.

The solar chimney, the actual thermal engine of the thermal power system, converts heat contained in the operating air into kinetic energy. The energy conversion is essentially determined by temperature rise of the ambient air entering the collector and chimney height.

The pressure difference, Δp, which is produced between the chimney air and the ambient, is calculated from [22]

$$\Delta p = g\int_0^H (\rho_a(h) - \rho(h))dh \tag{44}$$

where, g is the gravitational acceleration; H is chimney height; $\rho_a(h)$ and $\rho(h)$ are ambient air density and internal airflow density inside the chimney at any height h respectively.

By assuming a linear variation of air density with height, ΔP can further be written as,

$$\begin{aligned}\Delta p &= g\int_0^H(((\rho_{a1} - \rho_1) - (\beta_a - \beta)h))dh\\ &= g\cdot\left((\rho_{a1} - \rho_1)H - \frac{1}{2}(\beta_a - \beta)H^2\right)\end{aligned} \tag{45}$$

where, the mean gradient of ambient air density, β_a, is calculated according to the vertical temperature distribution [57]. The mean gradient of chimney inward air density, β, is calculated from,

$$\beta = \frac{\rho_2 - \rho_1}{H}. \tag{46}$$

The velocity of the airflow at the chimney inlet is given by [22],

$$u_1 = \sqrt{\frac{2(1-n)\Delta p}{\theta\cdot\rho_1}} \tag{47}$$

where n is factor of pressure drop at the turbine, which is assumed as a constant at 0.9 [28], and θ is the coefficient of total pressure loss including the entrance loss, exit kinetic energy loss, friction loss in the system [58].

3.3. Condensation in the condenser

Vapor contained in the warm and saturated air is condensed in the high-efficiency condenser installed at the chimney outlet.

The energy balance of warm and saturated air in the condenser, can be expressed by Wang et al. [53] as,

$$c_p\dot{m}_a(T_{3a}-T_{2a}) = c_p\dot{m}_f(T_2-T_3) + L_{con}\Delta\dot{m}_{water2} \tag{48}$$

where, T_{3a} is the temperature of ambient air flowing out from condenser; $\dot{m}_a$ is the mass flow of ambient air entering the condenser. The condensation of vapor to water in the high-efficiency condenser, $\Delta\dot{m}_{water2}$, can be expressed as,

$$\Delta\dot{m}_{water2} = \dot{m}_f\left(\frac{d_2}{1+d_2} - \frac{d_3}{1+d_3}\right). \tag{49}$$

3.4. Power output and conversion efficiency

The total electric power of CSCSPD, P_e, which includes one part $P_{e,ai}$ generated from the air turbine generators installed at the bottom of the chimney and another part $P_{e,wa}$ generated from the water generator installed outward from the bottom of the solar chimney, can be expressed as,

$$P_e = P_{e,ai} + P_{e,wa} \tag{50}$$

where, $P_{e,ai}$ and $P_{e,wa}$, are also given by,

$$P_{e,ai} = \eta_{ai} n A_{ch} u_1 \Delta P \tag{51}$$

$$P_{e,wa} = \eta_{wa}\Delta\dot{m}_{water2}\, gH \tag{52}$$

where, η_{ai} is the efficiency of air turbine generators recommended by Schlaich [22] as 80% and η_{wa} is the efficiency of water generator, which can reach 90%.

Total energy conversion efficiency of solar chimney system, η, can be expressed as the ratio of P_e to solar radiation radiated on solar collector,

$$\eta = \frac{P_e}{A_{coll}S}. \tag{53}$$

Based on the above elaborate model, a computation is done to predict and analyze the performances of the two systems.

4. Results and discussions

To obtain more heat used as the latent vapor heat and the heat energy contained in the upcurrent, a bigger collector is needed. Though super high chimneys more than 1000 m high can be constructed without any technical problem, moderately high chimneys around 500 m high are more practical. In this study, the combination of a chimney 500 m high and a collector 3000 m in radius is selected to be simulated and to evaluate the performance of CSCSPD. The surface air always contains some amount of dust. The dust contents of the air rising from the ground can be used as potential condensation nuclei. However, in reality, extra vapor contents in supersaturated upcurrent with certain velocity are not all condensed. In addition, the maximum theoretical quantity of condensed water is negligible. Therefore, all of the extra vapor contents in supersaturated air are assumed to be collected in the condenser in this work.

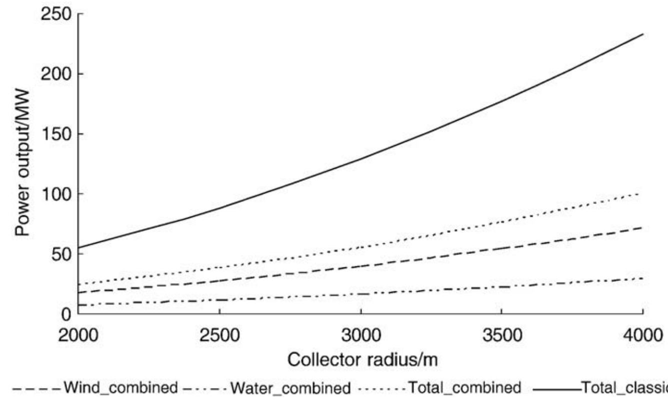

Fig. 3. Variations of power obtained from CSCSPD and CSCS with collector radius.

4.1. Validation

The chimney is the engine of airflow in the plant. Simulation of buoyancy — driven flow in high chimney being actually compressible flow [27] seems very important in the simulation using a model. In usual, the buoyancy — driven flow is treated as incompressible flow in simple simulations, whose results deviate from those calculated as incompressible flow to some extent [59,60].

Validation of the model for buoyancy — driven flow which rises by many meters is done in this work by comparing the data calculated using our model with those calculated by von Backström and Gannon [27] for CSCS. Table 1 presents the differences of the ratios of parametric performances including static pressure ratio, density, velocity and stagnation temperature at the outlet to those at the inlet using our model and von Backström et al.'s calculation for the classic solar chimney 300 m, 400 m, 500 m, 600 m, 700 m, 800 m, 900 m and 1000 m high by keeping other conditions constant at solar radiation of 1000 W m^{-2}.

As shown in Table 1, agreements within a difference of 3.4% for the ratios for classic solar chimneys with different heights are obtained. This strongly supports the idea that the model is exact for buoyancy — driven flow.

4.2. Performance

Table 2 shows the results calculated with the mathematical model for CSCSPD and CSCS with solar radiation of 1000 Wm^{-2}.

We note in Table 2 that the collector outlet airflow temperature for the CSCS is 26.8 °C higher than the corresponding temperature for the CSCSPD. This is because some of the heat is wasted in the vapor latent heat when the dry ambient air enters the collector inlet and becomes warm and saturated. In the collector, more heat is transferred into vapor latent heat, resulting in lower-velocity ventilation and a smaller power

Table 1
Comparison of performance simulated using our model and von Backström et al.'s calculation for classic solar chimneys with different heights.

Chimney height/m	300	400	500	600	700	800	900	1000
Difference of P_2/P_1 to von Backström et al.'s /%	0.86	1.20	1.54	1.89	2.26	2.63	3.01	3.40
Difference of Ma_2/Ma_1 to von Backström et al.'s /%	0.01	0.04	0.08	0.13	0.18	0.24	0.31	0.38
Difference of ρ_2/ρ_1 to von Backström et al.'s /%	0.01	0.04	0.08	0.13	0.19	0.24	0.31	0.38
Difference of T_{02}/T_{01} to von Backström et al.'s /%	0	0	0	0	0	0	0	0

Table 2
Performance of the proposed CSCSPD and CSCS.

Parameters	Value	Parameters	Value
Collector diameter/m	6000	Mass flow rate of saturated air (CSCSPD)/kg s^{-1}	166225
Chimney height/m	500	Collector outlet airflow temperature (CSCSPD)/°C	38.9
Chimney radius/m	80	Collector outlet airflow velocity (CSCSPD)/m s^{-1}	7.58
Collector outlet airflow temperature (CSCS)/°C	65.7	Total mass flow rate of vapor contained in the chimney inlet airflow (CSCSPD) /kg s^{-1}	7398.8
Collector outlet airflow velocity (CSCS)/m s^{-1}	11.5	Mass flow rate of condensed water in the condenser (CSCSPD)/kg s^{-1}	3807.1
Total power output (CSCS)/MW	128.8	Power output from air turbine generators (CSCSPD)/MW	39.2
Efficiency (CSCS)/%	0.46	Power output from water generators (CSCSPD)/MW	16.1
		Total power output (CSCSPD)/MW	55.3
		Efficiency (CSCSPD)/%	0.2

obtained from air turbine generators in the CSCSPD. The total power obtained from air turbine generators and water generators is also less than the power obtained from air turbine generators in the CSCS.

A calculation of power output is given here for the proposed plants running for 24 h every day, 365 days every year at a site with an annual global solar radiation of 1800 kWh m^{-2}. That is, average global solar radiation of 4.93 kWh m^{-2} will be received by the collector every day. Fig. 3 shows the comparisons of power outputs between the two plants as the output varies with collector radius. In this work, this chimney diameter is varied at the same rate as the collector's one. It can be seen from the figure that an increase in collector radius results in the increase in the power outputs of the two plants. This because the increase in collector radius induces the increase in temperature and vapor content of the airflow, thus producing an associated increase in power obtained from air turbine generators and water generators and an increase in fresh water output. This leads to the increase in fresh water revenue, as shown in Fig. 4. Moreover, the power output for the CSCSPD is throughout higher than the CSCS. The power obtained from water generators is far less than that obtained from air turbine generators.

Fig. 5 shows the comparisons of power outputs between the two plants with chimney height. In the figure, an increase in chimney height also results in an increase in the power outputs of the two plants. Airflow with larger velocity and lower temperature will be produced in the plant with higher chimney. This leads to the increase in power output from air turbine generators and that from water generators, and slight reduction in fresh water output, which results in slight reduction in fresh water revenue, as shown in Fig. 6.

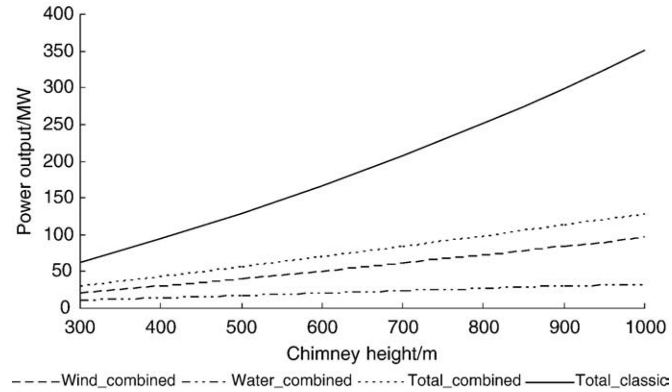

Fig. 5. Variations of power obtained from CSCSPD and CSCS with chimney height.

4.3. Revenue analysis

We conclude from the above analysis of performance that power output of CSCSPD is less than that of a CSCS with the same dimension under the same conditions. However, the CSCSPD produces the byproduct of fresh water, which can be supplied to consumers and local industries for use. The sale analysis of electricity per kWh and fresh water per ton are based on the price level in Dalian, China (Fresh water: 0.4 US \$ ton^{-1}; electricity: 0.09 US \$ kWh^{-1}. The following conversion rate for Yuan is used in this paper: Yuan 8 = US\$ 1). The two products are assumed to be used only for industrial purposes and not for domestic use.

The targets that a certain percentage of electricity is generated by renewable energy in future were established in many countries e.g. the European Union, the USA and Australia [61]. In fact, costs of electricity generated by renewable energy when incorporating additional revenue generated by carbon credits [62] are usually higher than levelised electricity cost of coal-fired power plants. The government targets may be implemented with several financial incentives, such as granting a subsidy per kW_{peak} capacity installed, implementing soft loans programmes, implementing soft taxes programmes, and being paid per kWh fed into the grid with a price above the market level at its site [61,63,64].

The levelised electricity cost of 100 MW solar chimney power plant proposed by Schlaich et al. (it reaches at 0.09 Euro per kWh electric power without incorporating additional revenue generated by carbon credits) [24] when incorporating additional revenue generated by carbon credits [62] is a little above that of coal-fired power

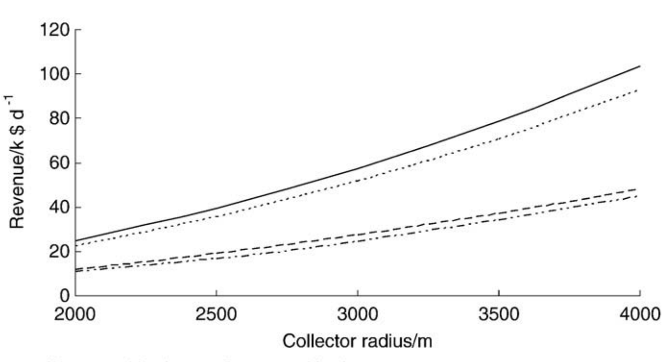

Fig. 4. Variations of revenue with collector radius for CSCSPD and CSCS.

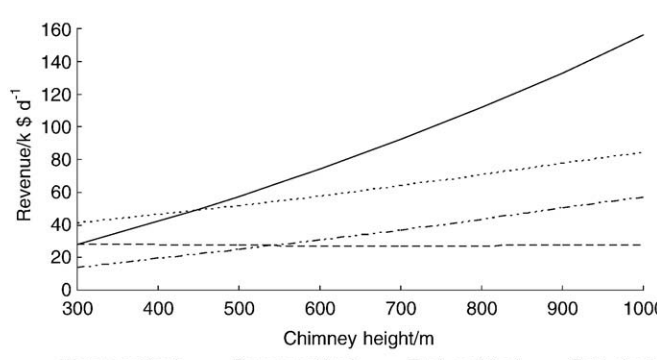

Fig. 6. Variations of revenue with chimney height for CSCSPD and CSCS.

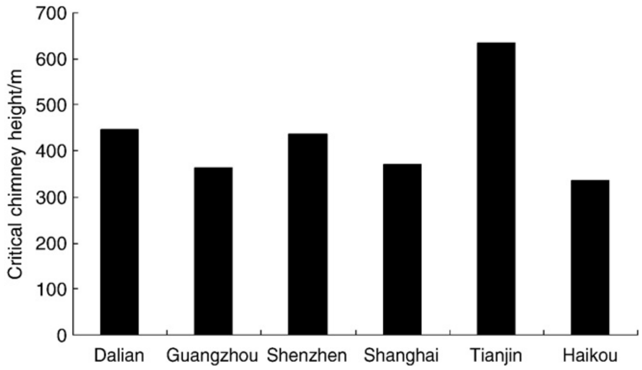

Fig. 7. Critical chimney height for the proposed solar chimney power plant at a site in several cities adjacent to the sea, in China.

plants. In this paper, the financial incentives to solar chimney power plants are assumed to include all the above incentives except the last one. In other words, the price of products i.e. electricity and fresh water will be paid at market level.

Figs. 5 and 6 show the variation of revenue from the two plants with collector radius and chimney height, respectively. The variations are consistent with those of the power output and the fresh water mass. The results show that the chimney less than 445 m high for the proposed combined solar chimney power plant having a collector 3000 m in radius is more economical than for the classic plant. Otherwise, CSCS is more economical.

Fig. 7 shows the critical chimney heights for the proposed solar chimney power plant having a collector 3000 m in radius at a site in several cities adjacent to the sea, in China. The recent prices of fresh water and electricity in the cities are presented in Table 3 [65]. We conclude that the critical chimney height depend on the price of fresh water and electricity. As shown in Fig. 7, with an increase in the ratio of the price of fresh water to the price of electricity, the critical chimney height increases.

5. Conclusions

A mathematical model has been developed for a one-dimensional compressible flow in CSCSPD and CSCS in this work. The performances of two different plants were investigated with the mathematical model, and the results were then compared. The following conclusions can be drawn from the analyses.

(1) The temperature and velocity of the airflow inside the combined chimney is far less than that inside the classic chimney since the vapor latent heat is released when air rises up the chimney.
(2) The power output of CSCSPD is less than that of the classic plant with the same dimension. It was also found that the power obtained from the water generator is far less than that obtained from the air turbine generators.
(3) A revenue analysis carried out comparing the electricity cost of the two plants based on the price level of fresh water and electric power in Dalian shows that the chimney less than 445 m high for the proposed combined solar chimney power plant having a collector 3000 m in radius is more economical than for the classic plant, otherwise, CSCS is more economical. From the analysis and results obtained, it is found that the critical chimney height depends on the price of fresh water and electricity.

Table 3
Prices of fresh water and electricity in several cities adjacent to the sea, in China [65].

	Price/$ per kWh electricity	Price/$ per ton water
Guangzhou	0.10125	0.31625
Shenzhen	0.0975	0.4125
Shanghai	0.09125	0.3125
Tianjin	0.09	0.7
Dalian	0.09	0.4
Haikou	0.0675	0.2

Acknowledgements

Thanks to the comments of the reviewers. This research has been supported by the National Natural Science Foundation of China (No.50908094), the China Postdoctoral Science Foundation (No.20090451052) and the Youth Science Foundation for Huazhong University of Science and Technology (No.0124240015).

References

[1] E. Delyannis, Historic background of desalination and renewable energies, Solar Energy 75 (2003) 357–366.
[2] C.A. Dompros, G. Roumbas, Renewable energy driven desalination systems modeling, Journal of Cleaner Production 15 (2007) 449–464.
[3] M. Telkes, Solar distillation produces fresh water from seawater, MIT Solar Energy Conversion Project, Publication No. 22 (1951) 24.
[4] B. Bouchekima, A solar desalination plant for domestic water needs in arid areas of South Algeria, Desalination 153 (2003) 65–69.
[5] L. García-Rodríguez, J. Blanco-Gálvez, Solar-heated Rankine cycles for water and electricity production: POWERSOL project, Desalination 212 (2007) 311–318.
[6] L. García-Rodríguez, A.M. Delgado-Torres, Solar-powered Rankine cycles for fresh water production, Desalination 212 (2007) 319–327.
[7] D. Alarcón-Padilla, L. García-Rodríguez, J. Blanco-Gálvez, Assessment of an absorption heat pump coupled to a multi-effect distillation unit within AQUASOL project, Desalination 212 (2007) 303–310.
[8] M. Reali, Solar barometric distillation for seawater desalting Part IV: Analyses of one-effect and two-effect distillation technologies, Desalination 212 (2007) 219–237.
[9] Y.M. El-Sayed, The rising potential of competitive solar desalination, Desalination 216 (2007) 314–324.
[10] A.M. Delgado-Torres, L. García-Rodríguez, Double cascade organic Rankine cycle for solar-driven reverse osmosis desalination, Desalination 216 (2007) 306–313.
[11] A.M. Delgado-Torres, L. García-Rodríguez, Comparison of solar technologies for driving a desalination system by means of an organic Rankine cycle, Desalination 216 (2007) 276–291.
[12] A.M. Delgado-Torres, L. García-Rodríguez, Preliminary assessment of solar organic Rankine cycles for driving a desalination system, Desalination 216 (2007) 252–275.
[13] H. Tanaka, Y. Nakatake, Improvement of the tilted wick solar still by using a flat plate reflector, Desalination 216 (2007) 139–146.
[14] M. Telkes, Solar stills, Proc. World Symposium on Applied Solar Energy (1956) 73–79.
[15] A. Delyannis, The Patmos solar distillation plant, Solar Energy 11 (1968) 113–115.
[16] P.I. Cooper, Solar distillation, Solar energy progress in Australia and New Zealand. Publication of the Australian and New Zealand Section of Solar Energy 8 (1969) 45.
[17] A.M. El-Nashar, The Abu Dhabi solar distillation plant, Desalination 52 (1985) 217–234.
[18] M. Collares-Pereira, J.F. Mendesa, P. Horta, Advanced solar dryer for salt recovery from brine effluent of desalination MED plant, Proc. ISES Solar World Congress 2003, Göteborg, Sweden, 2003.
[19] M. Collares-Pereira, J.F. Mendesa, P. Horta, Advanced solar dryer for salt recovery from brine effluent of desalination MED plant, Proc. EuroSun2004 — the 5th ISES Europe Solar Conference, Freiburg, Germany, 2004, 20–23 June.
[20] M. Collares-Pereira, J.F. Mendesa, P. Horta, N. Korovessis, Final design of an advanced solar dryer for salt recovery from brine effluent of an MED desalination plant, Desalination 211 (2007) 222–231.
[21] H. Günther, hundert Jahren — Die künftige Energieversorgung der Welt, Kosmos, Gesellschaft der Naturfreunde, Franckh'sche Verlagshandlung, Stuttgart, 1931.
[22] J. Schlaich, The solar chimney: Electricity from the sun, Edition Axel Menges, Stuttgart, Germany, 1995.
[23] J. Schlaich, R. Bergermann, W. Schiel and G. Weinrebe, Sustainable Electricity Generation with Solar Updraft Towers. Structural Engineering International, 3 (2004).
[24] J. Schlaich, R. Bergermann, W. Schiel, G. Weinrebe, Design of commercial solar updraft tower systems-utilization of solar induced convective flows for power generation, Journal of Solar Energy Engineering 127 (2005) 117–124.
[25] L.B. Mullet, The solar chimney overall efficiency, design and performance, International Journal of Ambient Energy 8 (1) (1987) 35–40.
[26] N. Pasumarthi, S.A. Sherif, Experimental and theoretical performance of a demonstration solar chimney model—Part I: Mathematical model development, International Journal of Energy Research 22 (1998) 277–288.

[27] T.W. von Backström, A.J. Gannon, Compressible flow through solar power plant chimneys, Journal of Solar Energy Engineering 122 (2000) 138–145.
[28] M.A. dos S. Bernardes, A. Voss, G. Weinrebe, Thermal and technical analyzes of solar chimneys, Soler Energy 75 (2003) 511–524.
[29] T.W. von Backström, A. Bernhardt, A.J. Gannon, Pressure drop in solar power plant chimneys, Journal of Solar Energy Engineering 125 (2003) 165–169.
[30] D. Bonnelle, Solar Chimney, water spraying Energy Tower, and linked renewable energy conversion devices: presentation, criticism and proposals. Doctoral thesis, University Claude Bernard-Lyon 1, France; July, 2004. Registration Number: 129–2004.
[31] H. Pastohr, O. Kornadt, K. Gurlebeck, Numerical and analytical calculations of the temperature and flow field in the upwind power plant, International Journal of Energy Research 28 (2004) 495–510.
[32] C.D. Papageorgiou, Floating Solar Chimney Technology, accessed at: http://www.floatingsolarchimney.gr, 2004.
[33] C.D. Papageorgiou, External wind effects on floating solar chimney, 4th IASTED Int. Conf. on Power and Energy Systems, Rhodes, Greece, 2004, pp. 159–163.
[34] C.D. Papageorgiou, Optimum Design for Solar Power Stations with Floating Solar Chimneys, ISES Asia Pacific Solar Energy Conf, Kwangju, Korea, 2004, pp. 763–772.
[35] E. Bilgen, J. Rheault, Solar chimney power plants for high latitudes, Soler Energy 79 (2005) 449–458.
[36] J.P. Pretorius, D.G. Kröger, Critical evaluation of solar chimney power plant performance, Soler Energy 80 (2006) 535–544.
[37] T.W. von Backström, T.P. Fluri, Maximum fluid power condition in solar chimney power plants—An analytical approach, Solar Energy 80 (2006) 1417–1423.
[38] F.N. Onyango, R.M. Ochieng, The potential of solar chimney for application in rural areas of developing countries, Fuel 85 (2006) 2561–2566.
[39] N. Ninic, Available energy of the air in solar chimneys and the possibility of its ground-level concentration, Solar Energy 80 (2006) 804–811.
[40] X.P. Zhou, J.K. Yang, B. Xiao, G.X. Hou, Experimental study of the temperature field in a solar chimney power setup, Applied Thermal Engineering 27 (2007) 2044–2050.
[41] X.P. Zhou, J.K. Yang, B. Xiao, G.X. Hou, Simulation of a pilot solar chimney power equipment, Renewable Energy 32 (2007) 1637–1644.
[42] X.P. Zhou, J.K. Yang, B. Xiao, X.Y. Shi, Special climate around a commercial solar chimney power plant, Journal of Energy Engineering, Transaction of ASCE 134 (2008) 6–14.
[43] X.P. Zhou, J.K. Yang, A novel solar thermal power plant with floating chimney stiffened onto a mountain-side and potential of the power generation in China's deserts, Heat Transfer Engineering 30 (2009) 400–407.
[44] X.P. Zhou, J.K. Yang, F. Wang, B. Xiao. Economic analysis of floating solar chimney power plant. Renewable and Sustainable Energy Reviews 13 (2009) 736–749.
[45] X.P. Zhou, J.K. Yang, J.B. Wang, B. Xiao. Novel concept for producing energy integrating a solar collector with a man made mountain hollow. Energy Conversion and Management 50 (2009) 847–854.
[46] W. Haaf, K. Friedrich, G. Mayr, J. Schlaich, Solar chimneys, part I: Principle and construction of the pilot plant in Manzanares, International Journal of Solar Energy 2 (1983) 3–20.
[47] W. Haaf, Solar chimneys, part II: Preliminary test results from the Manzanares pilot plant, International Journal of Solar Energy 2 (1984) 141–161.
[48] R.J.K. Krisst, Energy transfer system, Alternative Sources of Energy 63 (1983) 8–11.
[49] H. Kreetz, Theoretische Untersuchungen und Auslegung eines temporaren Wasserspeichers fur das Aufwindkraftwerk. Diplomarbeit. Energie und Verfahrenstechnik der TU Berlin, 1997.
[50] N. Pasumarthi, S.A. Sherif, Experimental and theoretical performance of a demonstration solar chimney model—Part II: Experimental and theoretical results and economic analysis, International Journal of Energy Research 22 (1998) 443–461.
[51] C. Ketlogetswe, J.K. Fiszdon, O.O. Seabe. Solar chimney power generation project – The case for Botswana. Renewable and Sustainable Energy Reviews 12 (2008) 2005–2012.
[52] C.B. Maia, A.G. Ferreira, R.M. Valle, M.F.B. Cortez. Theoretical evaluation of the influence of geometric parameters and materials on the behavior of the airflow in a solar chimney. Computers and Fluids 38 (2009) 625–636.
[53] Y.P. Wang, Z.L. Fang, L. Zhu, Z.Y. Yang, J.H. Wang, L.J. Han, Study on the integrated utilization of seawater by solar chimney, Acta Energiae Solaris Sinica 27 (2006) 382–387, in Chinese.
[54] W.C. Swinbank, Long-wave radiation from clear skies, Quarterly Journal of the Royal Meteorological Society 89 (1963) 339.
[55] S.Z. Zhou, R.Y. Zhang, C. Zhang, Meteorology and meteorology, 3rd edn, Higher Education Press, Beijing, China, 1997.
[56] V.V.N. Kishore, V. Joshi, A practical collector efficiency equation for non-convecting solar ponds, Solar Energy 33 (5) (1984) 391–395.
[57] H.Z. Zhao, Engineering fluid mechanics, Huazhong University of Science and Technology Press, Wuhan, China, 2005.
[58] G.L. Xu, X.M. Wang, T.H. Wu, W.H. Chen, Engineering heat transfer, China Electric Power Press, Beijing, China, 2005.
[59] X.P. Zhou, J.K. Yang, J.B. Wang, B. Xiao, G.X. Hou, Y.Y. Wu, Numerical investigation of a compressible flow through solar chimney, Heat Transfer Engineering 30 (2009) 670–676.
[60] X.P. Zhou, J.K. Yang, R.M. Ochieng, B. Xiao. Numerical investigation of a plume from a power generating solar chimney in an atmospheric cross flow. Atmospheric Research 91 (2009) 26–35.
[61] D.L. Talavera, G. Nofuentes, J. Aguilera, M. Fuentes, Tables for the estimation of the internal rate of return of photovoltaic grid-connected systems, Renewable and Sustainable Energy Reviews 11 (2007) 447–466.
[62] PointCarbon. Addressed at: http://www.pointcarbon.com, 2007.
[63] J. Bernal-Agustín, R. Dufo-López, Economical and environmental analysis of grid connected photovoltaic systems in Spain, Renewable Energy 31 (2006) 1107–1128.
[64] F. Trieb, Competitive solar thermal power stations until 2010 — the challenge of market introduction, Renewable Energy 19 (2000) 163–171.
[65] Price of electricity and water for industrial purposes in several cities in China. Addressed at: http://www.hnpi.net/jbwd-1.htm, Feb, 2007.

Glossary

Symbols

A: Area, m^2;
c_p: Specific heat capacity of wet air, J kg^{-1} K^{-1};
d: Moisture content of wet air, or thickness of thermal resistance bed, m;
g: Gravitational acceleration, m s^{-2};
h: Any height, m, or convection heat transfer coefficient, W m^{-2} K^{-1};
H: Chimney height, m;
h_r: Radiation heat transfer coefficient, W m^{-2} K^{-1};
I: Specific enthalpy, J kg^{-1};
k: Thermal conductivity, W m^{-1} K^{-1};
L: Latent heat of water evaporation, J kg^{-1};
$\dot{m}$: Mass flow rate;
Ma: Mach number;
n: Factor of pressure drop at the turbine;
p: Static pressure, Pa;
P_e: Total electric power, or electric power from generators, W;
r: Any radius, m;
S: Solar radiation, Wm^{-2};
T: Static temperature, °C or K;
T_f: Mean static temperature of operating air in the collector, K;
T_0: Stagnation temperature, K;
u: Velocity in vertical direction, m s^{-1};
U: Heat loss coefficient, W m^{-2} K^{-1};
v: Velocity in radial direction, m s^{-1};
v_w: Ambient wind velocity, m s^{-1};

Greek symbols

α: Absorptivity;
β: Mean gradient of air density;
γ: Specific heat ratio, 1.4;
$\Delta\dot{m}_{water1}$: Mass flow rate of vapor condensed to water in the chimney, kg s^{-1};
$\Delta\dot{m}_{water2}$: Mass flow rate of vapor condensed to water in the high-efficiency condenser, kg s^{-1};
Δp: Total pressure difference in the chimney , Pa;
ΔQ: Total vapor latent heat released, W;
ε: Emissivity;
η: Total efficiency, or energy conversion efficiency of components, %;
θ: Coefficient of total pressure loss;
ρ: Density, kg m^{-3};
σ: Stefan–Boltzmann constant, 5.67×10^{-8}, W m^{-2} K^{-4};
τ: Transmissivity;

Subscripts

a: Ambient air;
ab: Absorber;
ai: Air turbine generators;
$a0$: Ambient air at 0m above sea level;
b: Bottom loss;
c: Cover;
ch: Chimney;
$coll$: Collector;
$coll,out$: Collector outlet;
d: Dry air;
f: Operating air;
g: Ground loss;
p: Plastic film;
r: Thermal resistance bed;
se: Seawater surface;
sky: Sky;
sv: Saturated vapor;
$sv0$: Saturated vapor pressure at 0 °C;
t: Top loss;
v, va: Vapor;
wa: Water generators or water layer in the collector;
$water$: Water;
wi: Air turbine generators;
1: Chimney inlet or plates e.g. transparent cover film;
2: Chimney outlet, or transparent plastic film;
3: Condenser outlet, or black absorber.